Advanced and Sustainable Technologies (ASET)
Volume 1, No 1, June 2022 [1-9]

Computational Fluid Dynamic Analysis of Thermal Characteristics on the PLCC Package: Influence of velocity and heat flux

Frankey Anak Lintang[1*]

[1]Faculty of Mechanical Engineering Technology, Universiti Malaysia Perlis, Perlis, Malaysia.

Received 1 November 2021, Revised 25 January 2022, Accepted 15 February 2022

ABSTRACT

Thermal management is essential in electronic components and devices. Overheating of the component leads to malfunction. This study investigates the effects of velocity and heat flux on the Plastic Leaded Chip Carrier (PLCC) during the thermal cooling process via simulation analysis. Computational fluid dynamics software simulated the cooling process of PLCC. The size of the PLCC used is 2.72 cm × 2.72 cm × 0.38 cm. The effect of heat flux and velocity on temperature distribution, flow pattern, and pressure distribution was studied. The findings indicated that as the approach air velocity increased, the temperature of the packages decreased. The result also shows that the static pressure decrease along with the package when the air velocity increases. The simulation results are expected to understand better the cooling process of PLCC in the thermal management of electronic components and devices.

Keywords: Computational fluid dynamic, thermal characteristic, simulation and modeling

1. INTRODUCTION

The electronic industry is currently focused on making products smarter, lighter, and smaller while reducing heat [1]. This trend necessitated the establishment of stringent packaging standards. In electronic packaging, thermal management is a critical issue. When temperatures exceed 70^{o}C, electronic components comprised of a silicon chip and an organic substrate generate heat. This issue can be resolved by limiting the distance between PLCCs. Two PLCCs were simulated and evaluated in a small wind tunnel. A gap of 0 cm, 1.5 cm, and 3.0 cm between Power line carrier communication (PLCC) was determined to be appropriate [2]. When electronic components are operated continuously for an extended period, the chip temperature can easily exceed 70^{o}C. This condition may cause electronic components to become damaged or overheated. That is why, more than three decades ago, a large number of researchers began studying thermal management.

Plotnik and Anderson [3] and Tucker and Paul [4] used computational fluid dynamics to optimize heat transfer in electronic devices. Chen and Wang [5] investigated laminar and turbulent forced convective flows across two sequentially heated blocks mounted on a single principal channel wall. Hong and Yuan [6] demonstrated that variation in the local heat transfer coefficient significantly affects the local temperature distribution. Hung and Fu [7] created a two-dimensional model to simulate viscous laminar flow, mixed convection, and conjugated heat transfer between parallel plates on an integrated circuit board. For electronic packages, the conjugate issue is critical. Jayakanthan et al. [8] used FLUENT™ to simulate conjugate heat transfer in a wind tunnel between single and dual packages mounted on a PCB. Other researchers built on this work by simulating multiple chips with a two-dimensional model.

*Corresponding author: keyfrank94@gmail.com

As demonstrated by Tso et al. [9], Young and Vafai [10], and Kim and Kim [11], there has been continued interest in determining junction temperature and thermal resistance.

The electronic industry expanded rapidly in 2007 as a result of advancements in electronic packaging and nanotechnology. Yusof et al. [12] investigated the packaging of PLCCs using two packages. Mazlan et al. [13] enhanced the previously published study on PLCC electronic packaging. They investigated the effect of PLCC packages by varying the air inlet velocity and chip power. Chip temperature is affected by various factors, including coolant velocity, chip power, and PLCC gap. The objective was to dissect the execution of two PLCC bundles mounted on a PCB in a couple of different configurations. The numerical simulations were performed in three dimensions using FLUENT 6.3 [14]. The experiments were conducted using an air chamber equipped with a spout at various airspeeds to replicate the constrained convection warm exchange phenomena. By varying the chip control, dividing the bundles, and approaching airspeeds, parameters such as intersection temperature, warm resistance, and top surface averaged Nusselt number have been considered for each bundle. The simulation model utilized an air chamber with a nozzle that exhausted uniform air velocity flow over two Plastic Leaded Chip Carriers (PLCC). The PLCC used is 2.72 cm × 2.72 cm × 0.38 cm in size. This dimension is comparable to the ones employed by Ramadhyani et al. [15]. The motherboard and two PLCCs were symmetrically placed in the air chamber.

In the current study, the cooling of the PLCC package was considered for the thermal analysis. The simulation was conducted by the computational fluid dynamics (CFD) method. Two independent parameters, which are inlet velocity and heat flux, were investigated. The inlet velocity ranged from 1-5 m/s, and 100-500 W/m^2 for heat flux were applied to the simulation. The results of pressure and temperature were studied in the analysis.

2. MATERIAL AND METHODS

The initial phase in CFD recreation of the warm execution is a preprocessor. SOLIDWORKS was employed to draw the model, plan the issue in geometric arrangement, and work the geometry. Before the liquid stream issues can be fathomed, it needs the space in which the stream happens to assess the arrangement. CFD software has made the liquid spaces and the network era in a particular area. FLUENT has been utilized to build the geometry of the tube-shaped with sought measurements. Three-dimensional geometry has been made and coincided with shaping the framework. In the 3D model, the tetrahedral fitting has been finished with components, as appears in Figure 1. The velocity-inlet, pressure-outlet, wall, and default interior have been defined. The grid was then exported as a mesh file for further simulation.

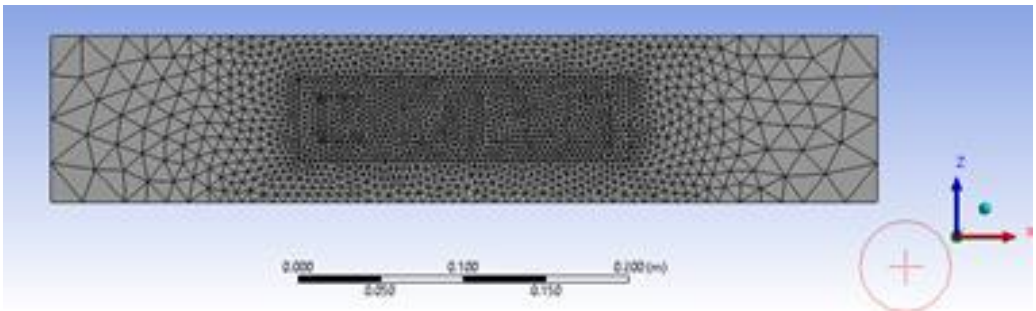

Figure 1: Geometry and mesh of PLCC packages.

The CFD solver does the stream estimations and techniques for the coveted outcomes. Familiar uses the limited volume strategy to comprehend the representing conditions for a liquid. It can utilize diverse physical models, for example, incompressible or compressible, inviscid or thick, laminar or turbulent [16]. Because administering conditions are non-straight and coupled, the solver performs several emphases on the arrangement circle before acquiring a unified arrangement, and the fundamental elements of the solver are based on the approximation of unknown flow variables using simple functions. Discretization is accomplished by substituting the approximation into the governing flow equations and subsequently manipulating the governing flow equations mathematically. The airflow was assumed to be laminar flow, incompressible and steady. The computation in the fluid domain for this study involves numerically solving Navier-Stokes equations. The mass conservation equation, also known as the continuity equation [17], is given by

Continuity equation:

$$\frac{\partial u}{\partial x}+\frac{\partial v}{\partial y}+\frac{\partial w}{\partial z}=0 \tag{1}$$

where u, v and w are the velocity vector in x, y and z directions, respectively. The momentum equations for Newtonian fluid in three dimensions are given by

Momentum equation:

$$\rho\left(\frac{\partial u}{\partial t}+u\frac{\partial u}{\partial x}+v\frac{\partial u}{\partial y}+w\frac{\partial u}{\partial z}\right)=-\frac{\partial P}{\partial x}+\mu\left(\frac{\partial^2 u}{\partial x^2}+\frac{\partial^2 u}{\partial y^2}+\frac{\partial^2 u}{\partial z^2}\right) \tag{2}$$

$$\rho\left(\frac{\partial v}{\partial t}+u\frac{\partial v}{\partial x}+v\frac{\partial v}{\partial y}+w\frac{\partial v}{\partial z}\right)=-\frac{\partial P}{\partial y}+\mu\left(\frac{\partial^2 v}{\partial x^2}+\frac{\partial^2 v}{\partial y^2}+\frac{\partial^2 v}{\partial z^2}\right) \tag{3}$$

$$\rho\left(\frac{\partial w}{\partial t}+u\frac{\partial w}{\partial x}+v\frac{\partial w}{\partial y}+w\frac{\partial w}{\partial z}\right)=-\frac{\partial P}{\partial z}+\mu\left(\frac{\partial^2 w}{\partial x^2}+\frac{\partial^2 w}{\partial y^2}+\frac{\partial^2 w}{\partial z^2}\right) \tag{4}$$

where ρ is the fluid density, P is the static pressure, and μ is the fluid viscosity. The energy equation that computes the heat generation and transfers in a non-isothermal environment is given by

Energy equation

$$\rho C_p\left(\frac{\partial T}{\partial t}+u\cdot\nabla T\right)=\nabla(k\nabla T) \tag{5}$$

where k is the thermal conductivity, C_p is the specific heat, and T is the temperature.

The boundary condition of the structural model has been defined at the bottom surfaces of the PLCC packages. All side surfaces were defined as the wall boundary other than the side inlet for velocity inlet entering from the x-axis and side outlet for pressure outlet. Inside the domain is fluid as the cell zone condition. Figure 2 shows the boundary conditions of the domain and the packages.

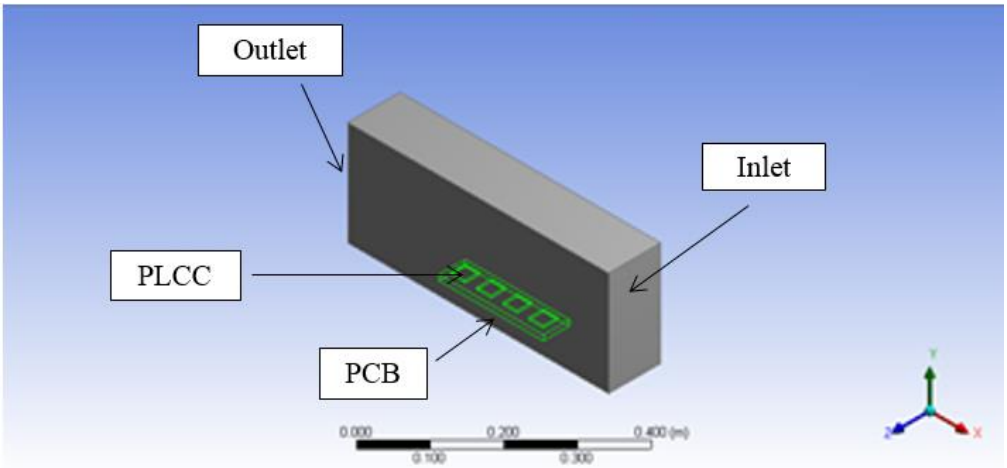

Figure 2: Boundary conditions.

3. RESULTS AND DISCUSSION

Figure 3 shows the relationship between the four packages' static temperature and heat flux. Generally, the results show that the temperature increases with heat flux. This situation indicates that high heat flux produces a high temperature. Amongst the PLCC package, PLCC 4 has the highest temperature. The static temperature of the PLCC 1-4 increases linearly when the heat flux rises by 100 W/m^2. The static temperature of PLCC 1 is lower because the air velocity hits it first after the air flows into the inlet. The air velocity entered and carried the heat away from the packages of PLCC 1 to PLCC 4. PLCC 2-4 increases due to less heat being carried away by the airflow in the cooling process. This phenomenon is clearly observed in the static temperature simulation contour (Figure 4).

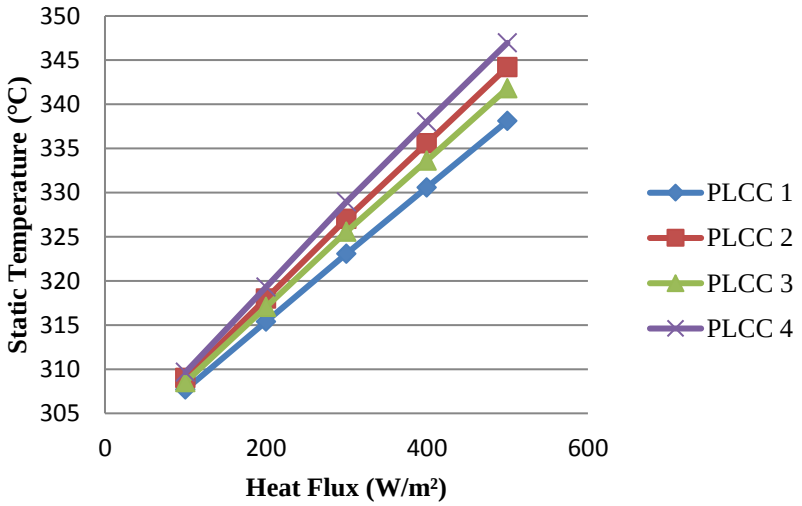

Figure 3: Variation of the static temperature of four packages with different heat fluxes.

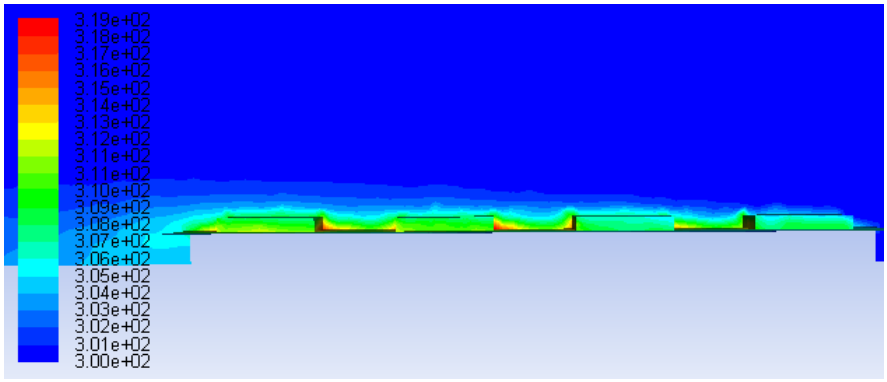

Figure 4: Contour of static temperature.

The air velocity is higher when entering the domain and spreads before it flows through the PLCC package. Figure 5 shows that PLCC 1 has the highest air velocity. The space between the PLCC has the lowest air velocity. The air velocity flowing through PLCC 1 is reversed back due to the frontal pressure at the packages. Therefore, less air velocity passes through PLCC 2 and increases again when it passes through the outlet. PLCC 4 has high velocity because the airflow through the surrounding is collected before throughout the packages. Figure 5 illustrates the velocity vector coloured by the air velocity.

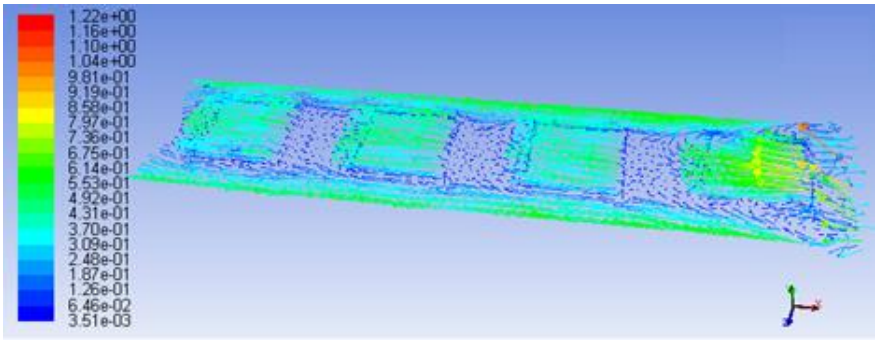

Figure 5: Velocity vectors coloured by the air velocity.

The rise of heat flux value crucially affects the temperature on the PLCC package. The significant effect of the heat flux can be observed in Figure 6 on the temperature contour. The results from two heat fluxes with similar inlet velocity were compared in Figure 6. The results show that both results have a similar temperature contour. However, the temperature value is higher for 500 W/m^2 of heat flux. Pressure and temperature contours were presented for 100 and 500 W/m^2 of heat flux. The static pressure with the different air velocities in the range of 1 to 5 m/s is presented in Figure 7. The results show that the static pressure decreased along with the PLCC package. The front region of the PLCC package experiences higher pressure due to the direct hitting from the airflow. However, the heat flux does not affect the pressure contour on the PLCC package. In Figure 7, the pressure value varied due to the changes in inlet velocity.

The pressure acting on the PLCC package decreased when the airflow through along the package (Figure 8). Figure 9 shows the relationship between the static temperature and the air velocity. The highest static temperature is PLCC 4, while the lowest is PLCC 1. Generally, the temperature decrease with the increase of velocity. The results show that all packages have decreased in temperature value in increasing the velocity.

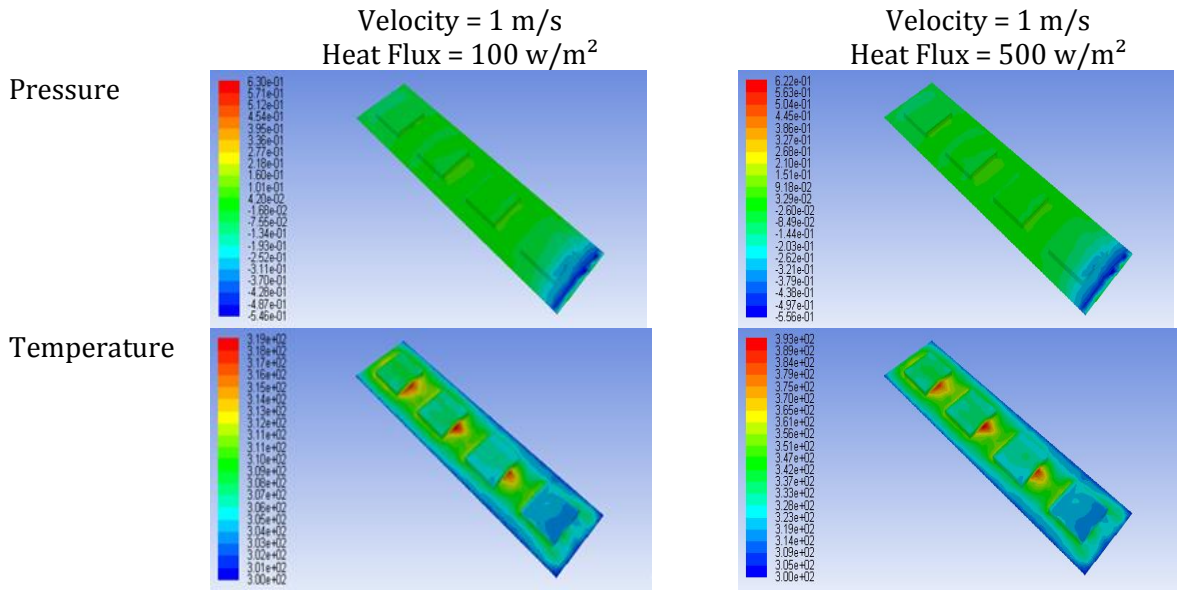

Figure 6: Contour of the PLCC packages on the air velocity of 1 m/s and heat flux of 100 and 500 w/m^2.

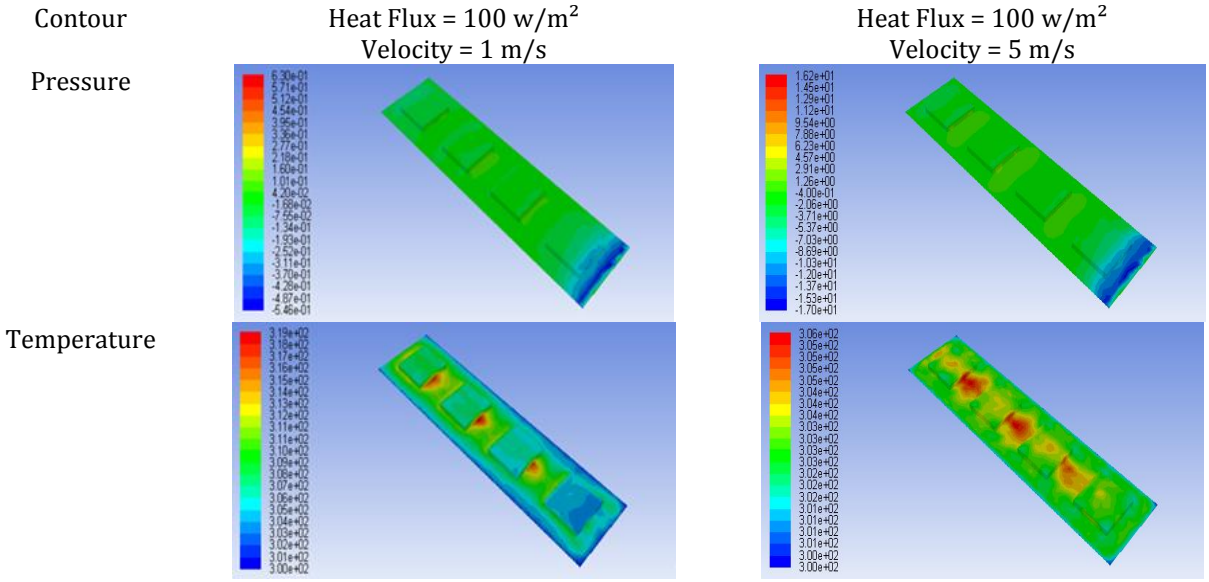

Figure 7: Contour of the PLCC packages at a heat flux of 100 w/m^2 and air velocity of 1 and 5 m/s.

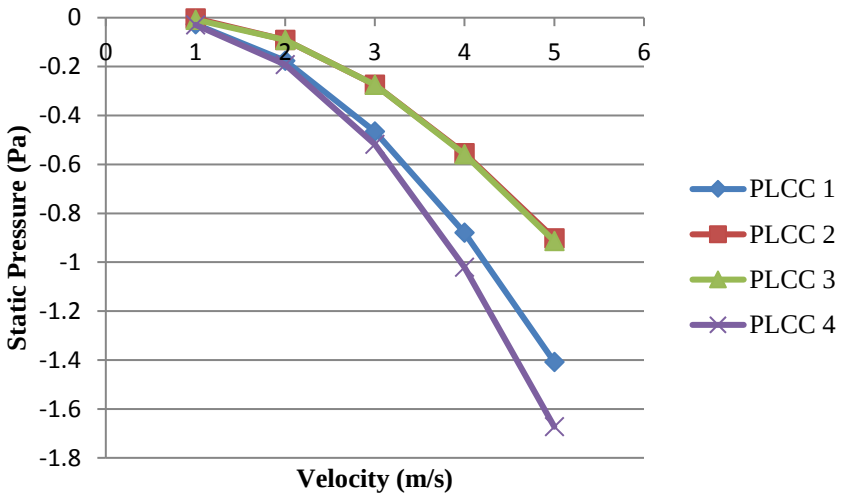

Figure 8: Variation of the static pressure of PLCC packages with different air velocities.

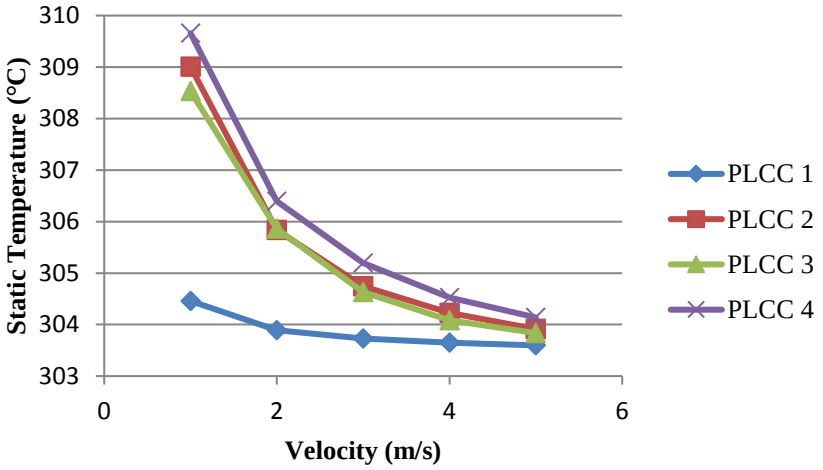

Figure 9: Variations of the static temperature of PLCC packages with different air velocities.

4. CONCLUSION

The effect of heat flux and inlet velocity on the PLCC packages has been studied. The static temperature and pressure were investigated by increasing the heat flux. The thermal characteristics of PLCC packages are influenced by the heat source on the plate surface as well as the air velocity passing through the PLCC. The effect of air velocity on the temperature of the PLCC packages during the cooling process is related to the temperature of the packages. The increase in air velocity may carry more heat away from the PLCC packages, lowering the component's temperature. The results revealed the linear behaviour of the temperature and the heat flux of PLCC. The investigation of the thermal performance of the PLCC packages may be extended to different designs, arrangements, and sizes. This CFD simulation analysis is expected to explain the cooling of the PLCC package.

REFERENCES

[1] Lam Po Tang, S. Recent developments in flexible wearable electronics for monitoring applications. Transactions of the Institute of Measurement and Control, vol 29, issue 3-4 (2007) pp.283-300.

[2] Yusoff, S., Mohamed, M., Ahmad, K. A., Abdullah, M. Z., Mujeebu, M. A., Ali, Z. M., & Yaakob, Y. 3-D conjugate heat transfer analysis of PLCC packages mounted in-line on a Printed Circuit Board. International Communications in Heat and Mass Transfer, vol 36, issue 8 (2009) pp.813-819.

[3] Plotnik, A. M., & Anderson, A. M. Using computational fluid dynamics to design heat transfer enhancement methods for cooling channels. In International Design Engineering Technical Conferences and Computers and Information in Engineering Conference. vol 17018, (1995). pp.341-350.

[4] Tucker, P. G. CFD applied to electronic systems: a review. IEEE Transactions on Components, Packaging, and Manufacturing Technology: Part A, vol 20, issue 4 (1997) pp.518-529.

[5] Chen, Y. M., & Wang, K. C. Experimental study on the forced convective flow in a channel with heated blocks in tandem. Experimental Thermal and Fluid Science, vol 16, issue 4 (1998) pp.286-298.

[6] Hong, B. Z., & Yuan, T. D. Heat transfer and nonlinear thermal stress analysis of a convective surface mount package. IEEE Transactions on Components, Packaging, and Manufacturing Technology: Part A, vol 20, issue 2 (1997) pp.213-219.

[7] Hung, T. C., & Fu, C. S. Conjugate heat transfer analysis for the passive enhancement of electronic cooling through geometric modification in a mixed convection domain. Numerical Heat Transfer: Part A: Applications, vol 35, issue 5 (1999) pp.519-535.

[8] Jayakanthan, A., Hassan, A. Y., & Seetharamu, K. N. Application of CFD in cooling electronic packages. In The Seventh Asian Congress of Fluid Mechanics. (1997) pp.777-780.

[9] Tso, C. P., Xu, G. P., & Tou, K. W. An experimental study on forced convection heat transfer from flush-mounted discrete heat sources. Journal of heat transfer, vol 121, issue 2 (1999) pp.326-332.

[10] Young, T. J., & Vafai, K. Experimental and numerical investigation of forced convective characteristics of arrays of channel mounted obstacles. Journal of heat transfer, vol 121, issue 1 (1999) pp.34-42.

[11] Kim, S., & Kim, D. Forced convection in microstructures for electronic equipment cooling. *Journal of heat transfer*, vol 121, issue 3 (1999) pp.639-645.

[12] Yusoff, S., Mohamed, M., Ahmad, K. A., Abdullah, M. Z., Mujeebu, M. A., Ali, Z. M., ... & Yaakob, Y. 3-D conjugate heat transfer analysis of PLCC packages mounted in-line on a Printed Circuit Board. International Communications in Heat and Mass Transfer, vol 36, issue 8 (2009) pp.813-819.

[13] Mazlan, M., Atan, R., Al Bakri Abdullah, M. M., Ahmad, M. I., Yusoff, M. H., & Saad, F. N. A. Three dimensional simulation of thermal pad using nanomaterial, nanosilver in semiconductor and electronic component application. In Advanced Materials Research. vol. 626 (2013) pp.980-988.

[14] Ong, E. E., Abdullah, M. Z., Khor, C. Y., Loh, W. K., Ooi, C. K., & Chan, R. Analysis of encapsulation process in 3D stacked chips with different microbump array. International communications in heat and mass transfer, vol 39, issue 10 (2012) pp.1616-1623.

[15] Ramadhyani, S., Moffatt, D. F., & Incropera, F. P. Conjugate heat transfer from small isothermal heat sources embedded in a large substrate. International Journal of Heat and Mass Transfer, vol 28, issue 10 (1985) pp.1945-1952.

[16] Aziz, M. S. A., Abdullah, M. Z., & Khor, C. Y. Influence of PTH offset angle in wave soldering with thermal-coupling method. Soldering & Surface Mount Technology. vol 26, issue 3 (2014) 97-109.

[17] Khor, C., Abdullah, M., & Mujeebu, M. A. Influence of Gap Height in Flip Chip Underfill Process With Non-Newtonian Flow Between Two Parallel Plates. Journal of electronic packaging, vol 134, issue 1, (2012) pp.011003.